Journal of Structural Engineering, *ASCE*, Vol. 126, No. 11, pp. 1356-1363, 2000.

Structural Health Monitoring using Statistical Process Control

Hoon Sohn[1], Jerry J. Czarnecki[2], and Charles R. Farrar, P.E., Fellow, ASCE[3]

This paper poses the process of structural health monitoring in the context of a statistical pattern recognition paradigm. This paper particularly focuses on applying a statistical process control technique known as "X-bar control chart" to vibration-based damage diagnosis. A control chart provides a statistical framework for monitoring future measurements and for identifying new data that are inconsistent with past data. First, an auto-regressive (AR) model is fit to the measured time histories from an undamaged structure. Coefficients of the AR model are selected as the damage-sensitive features for the subsequent control chart analysis. Next, control limits of the X-bar control chart are constructed based on the features obtained from the initial structure. Finally, the AR coefficients of the models fit to subsequent new data are monitored relative to the control limits. A statistically significant number of features outside the control limits indicate a system transition from a healthy state to a damage state. A unique aspect of this study is the coupling of various projection techniques such as principal component analysis, linear and quadratic discriminant operators with the statistical process control in an effort to enhance the discrimination between features from the undamaged and damaged structures. This combined statistical procedure is applied to vibration test data acquired from a concrete bridge column as the column is progressively damaged. The coupled approach captures a clearer distinction between undamaged and damaged vibration responses than applying a statistical process control alone.

KEY WORD: statistical process control, structural health monitoring, control chart, projection techniques, statistical pattern recognition, bridge column, time series analysis, and damage detection.

[1] Postdoctoral Research Fellow, ESA-EA, Los Alamos National Laboratory, Los Alamos, NM 87545.
[2] Ph.D. student, Dept. of Civil and Environmental Eng., MIT, Cambridge, MA 02139.
[3] Materials Behavior Team Leader, ESA-EA, Los Alamos National Laboratory, Los Alamos, NM 87545.

1. INTRODUCTION

Many aerospace, civil, and mechanical engineering systems continue to be used despite aging and the associated potential for damage accumulation. Therefore, the ability to monitor the structural health of these systems is becoming increasingly important from both economic and life-safety viewpoints. Damage identification based upon changes in dynamic response is one of the few methods that monitor changes in the structure on a global basis. The basic premise of vibration-based damage detection is that changes in the physical properties, such as reductions in stiffness resulting from the onset of cracks or loosening of a connection, will cause changes in the measured dynamic response of the structure.

Structural health monitoring has received considerable attention in the technical literature where there has been a concerted effort to develop a firm mathematical and physical foundation for this technology. Doebling et al. (1998) present a recent thorough review of vibration-based structural health monitoring methods. Because all vibration-based damage detection processes rely on experimental data with its inherent uncertainties, statistical analysis procedures are necessary if one is to state in a quantifiable manner that changes in the vibration response of a structure are indicative of damage as opposed to operational, and/or environmental variability. However, most references cited in this review focus on different methods for extracting damage-sensitive features from vibration response measurements. Few of the cited references take a statistical approach to quantifying the observed changes in these features.

This paper casts the structural health-monitoring problem in the context of a statistical pattern recognition paradigm. This paradigm can be described as a four-part process: 1.) operational evaluation, 2.) data acquisition & cleansing, 3.) feature extraction & data reduction, and 4.) statistical model development. In particular, this paper focuses on Parts 3 and 4 of the process and these portions are discussed in detail below. More detailed discussion of the statistical pattern recognition

paradigm can be found in Farrar and Doebling (1999). The process is illustrated through application to time history data measured on undamaged and subsequently damaged concrete columns. Note that the primary objective of this study is to identify the existence of damage. The localization and quantification of damage are not addressed in this study.

2. SPATIAL DATA COMPRESSION

The distinction between feature extraction and data reduction is not always clear cut. Feature extraction is the process of identifying damage-sensitive properties from the measured vibration response, and this process often results in some form of data reduction. Data compression into feature vectors of small dimension is necessary if accurate estimates of the feature statistical distribution are to be obtained. The need for low dimensionality in the feature vectors is referred to as the "curse of dimensionality" and is discussed in general texts on density function estimation (Scott 1992).

In this study, principal component analysis (PCA) is used to perform data compression prior to the feature extraction process when data from multiple measurement points are available. This process transforms the time series from multiple measurement points into a single time series preserving as much of relevant information as possible during the dimensionality reduction.

If $u_i(t_j)$ ($i = 1,..,\ m$ and $j=1,..,\ l$), denotes the response time histories corresponding to m measurement locations and sampled at l time intervals, a vector of the response components corresponding to the m measurement locations is formed at a given time, t_j, as:

$$\mathbf{u}(t_j) = \left[u_1(t_j) \quad u_2(t_j) \cdots u_m(t_j) \right]^T \tag{1}$$

where, each time history is first normalized by subtracting it mean value. Then, the $m \times m$ covariance matrix, Ω, among spatial measurement locations summed over all time samples is given by

$$\Omega = \sum_{j=1}^{l} \mathbf{u}(t_j)\,\mathbf{u}(t_j)^{\mathrm{T}} \tag{2}$$

The eigenvalues, λ_i, and eigenvectors, $\mathbf{v}_i$, of the covariance matrix satisfy:

$$\Omega\,\mathbf{v}_i = \lambda_i \mathbf{v}_i \tag{3}$$

Here, an eigenvector $\mathbf{v}_i$ is also called a *principal component*. To reduce the *m*-dimensional vector $\mathbf{u}(t)$ into a *d*-dimensional vector, $\mathbf{x}_v(t)$, where $d < m$, $\mathbf{u}(t)$ is projected onto the eigenvectors corresponding to first *d* largest eigenvalues:

$$\mathbf{x}_v(t) = [\mathbf{v}_1 \quad \cdots \quad \mathbf{v}_d]^{\mathrm{T}}\,\mathbf{u}(t) \tag{4}$$

For the examples presented in Section 6.8, all time histories from the measurement points are projected onto the first principal component.

3. FEATURE EXTRACTION

Feature extraction is the process of the identifying damage-sensitive properties derived from the measured vibration response that allows one to distinguish between the undamaged and damaged structures. Typically, systematic differences between time series from the undamaged and damaged structures are nearly impossible to detect by eye. Therefore, other features of the measured data must be examined for damage detection.

In this study, the coefficients of auto-regressive (AR) models are selected as damage sensitive features. The time series from an individual measurement point, or the spatially-compressed time series obtained from PCA, can be used to construct the AR models. In the AR(*n*) model the current point in a time series is modeled as a linear combination of the previous *n* points:

$$y(t) = \sum_{j=1}^{n} \phi_j \; y(t-j) \; + e(t) \;, \tag{5}$$

where y(t) is the time history at time t, ϕ_j is an unknown auto-regression coefficient, and e(t) is an random error with zero mean and constant variance. The ϕ_j's are estimated by fitting the AR model to the time history data using the Yule-Walker method (Brockwell and Davis 1991). A detailed discussion on AR model order selection can be found in Box et al. (1994).

For the application reported herein, the time signals are divided into smaller size time windows, and AR coefficients are estimated from each time window. Following this procedure, a large set of AR coefficients are obtained for subsequent damage diagnoses. As mentioned earlier, it is desirable to obtain many samples of the selected features for statistical analysis.

4. DATA COMPRESSION FOR FEATURE VECTOR DISCRIMINATION

Section 3 described methods for obtaining an *n*-dimensional feature space of AR coefficients. In such situation where multi-dimensional feature vectors exist, several monitoring procedures may be employed for feature vector discrimination. For example, each AR coefficient can be monitored by a variety of statistical procedures, or simultaneous monitoring of all AR coefficients can be done using multivariate statistical procedures. However, for feature vectors with a high dimensionality, the first approach can result in a large amount of data to be monitored and the visualization of the multivariate data can be very difficult. In this study the multi-dimensional feature vectors are projected onto one-dimensional subspaces and the statistical discrimination procedure is applied to the one-dimensional variable. Two transformations, linear and quadratic projections, are presented to maximize the separation in features from the undamaged and damaged structures.

In order to derive specific linear and quadratic projections, consider a situation in which there are only two classes (classes A and B) and multi-dimensional feature vector **x** is obtained. Fukunaga (1990) shows that a decision boundary, $\mathrm{D}(\mathbf{x})$, based on Bayes' Theorem minimizes the probability of

error, which is the probability of misclassification of assigning a new feature to class A when, in fact, it belongs to class B, or vice versa.

If classes A and B have normal distributions, the Bayes decision rule, $\mathrm{D}(\mathbf{x})$, can be written in a quadratic form (Fukunaga 1990):

$$\mathrm{D}(\mathbf{x}) = \mathbf{x}^{\mathrm{T}}\mathbf{Q}\,\mathbf{x} + \mathbf{V}\mathbf{x} \tag{6}$$

where **Q** is a quadratic projection matrix and **V** is a linear projection. In the case where the covariance matrices for classes A and B are identical matrices, the classification boundary can be further simplified to a linear form:

$$\mathrm{D}(\mathbf{x}) = \mathbf{F}^{\mathrm{T}}\mathbf{x} \tag{7}$$

The **Q, V,** and **F** matrices will be estimated later in this section.

The decision rule can be also viewed as a projection that maps multi-dimensional space $\mathbf{x}$ to one-dimensional space $\mathrm{D}(\mathbf{x})$. We are particularly interested in defining a transformed feature $\tau = \mathrm{D}(\mathbf{x})$ such that the means of two classes are as far as possible and their variances are the smallest as possible after either quadratic or linear projection. These projections can be sought by maximizing the following Fisher criterion (Bishop 1995):

$$f = \frac{(\mathrm{m}_{\mathrm{A}} - \mathrm{m}_{\mathrm{B}})^2}{\sigma_{\mathrm{A}}^2 + \sigma_{\mathrm{B}}^2} = \frac{\mathbf{F}^{\mathrm{T}}(\mathbf{m}_{\mathrm{A}} - \mathbf{m}_{\mathrm{B}})(\mathbf{m}_{\mathrm{A}} - \mathbf{m}_{\mathrm{B}})^{\mathrm{T}}\mathbf{F}}{\mathbf{F}^{\mathrm{T}}(\mathbf{\Sigma}_{\mathrm{A}} + \mathbf{\Sigma}_{\mathrm{B}})\mathbf{F}} \tag{8}$$

where $\mathbf{m}_{\mathrm{A}}$ and $\mathbf{m}_{\mathrm{B}}$ are the mean vectors of the classes A and B distributions. $\mathbf{\Sigma}_{\mathrm{A}}$ and $\mathbf{\Sigma}_{\mathrm{B}}$ are the covariance matrices of each class. m_{A} and m_{B} are the means of the projected feature in classes A and B. σ_{A} and σ_{B} are the corresponding standard deviations of the transformed features, respectively. Furthermore, the moments of the projected feature are related to those of the multi-dimensional feature vector **x** as follows**:**

$$\mathrm{m}_i = \mathbf{F}^{\mathrm{T}}\mathbf{m}_i \quad \text{and} \quad \sigma_i^2 = \mathbf{F}^{\mathrm{T}}\,\mathbf{\Sigma}_i\,\mathbf{F} \quad \text{for} \quad i = \mathrm{A} \text{ or } \mathrm{B} \tag{9}$$

Taking derivatives of *f* with respect to $\mathbf{F}$ and setting this quantity equal to zero yields the following linear projection (Bishop 1995):

$$\mathbf{F} = 2(\mathbf{\Sigma}_{\mathrm{A}} + \mathbf{\Sigma}_{\mathrm{B}})^{-1}(\mathbf{m}_{\mathrm{A}} - \mathbf{m}_{\mathrm{B}}) \tag{10}$$

It is important to mention that the performance of the linear classifier will not be optimal unless $\mathbf{\Sigma}_{\mathrm{A}}$ and $\mathbf{\Sigma}_{\mathrm{B}}$ are the same. It is only under the assumption of equal covariance matrices that the decision role reduces to a linear one. For the test data employed in Section 6, acceleration data from undamaged and damaged classes are observed to have unequal covariance matrices. Because the Bayesian decision boundary is quadratic under the more general circumstance of unequal covariance matrices between classes, the quadratic transformation yields the best discrimination power. The calculation of the quadratic term $\mathbf{Q}$ and linear term $\mathbf{V}$ in Equation (6) is computationally more intensive than the linear case. However, introducing a new variable y_i, which represents the product of two x_i's, Equation (6) can be linearized in the following form (Fukunaga 1990):

$$\mathrm{D}(\mathbf{x}) = \sum_{i=1}^{n}\sum_{j=1}^{n} q_{ij}x_i x_j + \sum_{i=1}^{n} v_i x_i = \sum_{i=1}^{n(n+1)/2} a_i y_i + \sum_{i=1}^{n} v_i x_i \tag{11}$$

where q_{ij}, v_i are the components of $\mathbf{Q}$ and $\mathbf{V}$ respectively. y_i represents the product of the x_j's and a_i is the corresponding entry in the $\mathbf{Q}$ matrix. In addition, *n* is the order of the AR model or the dimension of AR coefficients defined in Equation (5).

Let $\mathbf{Y}$ and $\mathbf{X}$ denote column vectors of y_i's and x_j's, respectively. Now, the following equation analogous to the linear case can be solved for $\mathbf{Q}$ and $\mathbf{V}$ by introducing a new variables vector $\mathbf{Z} = [\mathbf{Y}^{\mathrm{T}}\ \mathbf{X}^{\mathrm{T}}]^{\mathrm{T}}$ and letting $\mathbf{E}$ and $\mathbf{S}$ be the expected vector and covariance matrix of $\mathbf{Z}$, respectively:

$$[a_1 \cdots\ a_{n(n+1)/2}\, v_1\ \cdots\ v_n]^{\mathrm{T}} = 2[\mathbf{S}_{\mathrm{A}} + \mathbf{S}_{\mathrm{B}}]^{-1}(\mathbf{E}_{\mathrm{A}} - \mathbf{E}_{\mathrm{B}}) \tag{12}$$

Then a_i's and v_j's can be rearranged to form the **Q** matrix and **V** vector. Note that the projection techniques presented here are used for a dimensionality reduction purpose as well as for a construction of a discriminant function. That is, the *n*-dimensional AR coefficient space is projected onto a single scalar space maximizing the mean differences between two classes. Damage diagnosis is conducted on the transformed feature using the statistical process control technique described in the following section.

5. STATISTICAL MODELING: STATISTICAL PROCESS CONTROL

Statistical model development is concerned with the implementation of the algorithms that analyze the distribution of extracted features to determine the damage state of the structure. The algorithms used in statistical model development fall into the three general categories: 1. Group Classification, 2. Regression Analysis, and 3. Outlier Detection. The appropriate algorithm to use will depend on the ability to perform *supervised* or *unsupervised* learning. Here, supervised learning refers to the case were examples of data from damaged and undamaged structures are available. Unsupervised learning refers to the case were data is only available from the undamaged structure. This paper focuses on unsupervised learning methods.

In this study control chart analysis, which is the most commonly used SPC technique and very suitable for automated continuous system monitoring, is applied to the selected features to investigate the existence of damage in the structure of interest. When the system of interest experiences abnormal conditions, the mean and/or variance of the extracted features are expected to change. Here an X-bar control chart is employed to monitor the changes of the selected feature means and to identify samples that are inconsistent with the past data sets. Application of the S control chart, which measures the variability of the structure over time, to the current test structure is

presented in Fugate et al. (2000). Several variations of the control charts can be found in Montgomery (1997). To monitor the mean variation of the features, the features (*i.e.*, the AR coefficients or the transformed feature after linear or quadratic projection) are first arranged in subgroups of size *p*. τ_{ij} is the *j*th feature from the *i*th subgroup. The subgroup size *p* is often taken to be 4 or 5 (Montgomery 1997). If *p* is chosen too large, a drift present in individual subgroup mean may be obscured, or averaged-out. An additional motivation for the using subgroups, as opposed to individual observations, is that the distribution of the subgroup mean values can be reasonably approximated by a normal distribution as a result of central limit theorem.

Next, the subgroup mean $\overline{\mathrm{X}}_i$ and standard deviation S_i of the features are computed for each subgroup ($i = 1, \cdots, q$: where *q* is the number of subgroups):

$$\overline{\mathrm{X}}_i = mean\left(\tau_{ij}\right) \text{ and } \mathrm{S}_i = std(\tau_{ij}) \tag{13}$$

Here, the mean and standard deviation are with respect to *p* observations in each subgroup. Finally, an X-bar control chart is constructed by drawing a centerline (CL) at the subgroup mean and two additional horizontal lines corresponding to the upper and lower control limits (UCL & LCL) versus subgroup numbers (or with respect to time). The centerline and two control limits are defined as follows:

$$\mathrm{UCL},\ \mathrm{LCL} = \mathrm{CL} \pm Z_{\alpha/2}\frac{\mathrm{S}}{\sqrt{n}}, \text{ and } \mathrm{CL} = mean(\overline{\mathrm{X}}_i), \tag{14}$$

where the calculation of mean is with respect to all subgroups ($i = 1, \cdots, q$). $Z_{\alpha/2}$ is the percentage point of the normal distribution with zero mean and unit variance such that $P[z \geq Z_{\alpha/2}] = \alpha/2$. The variance S^2 is estimated by averaging the variance S_i^2 of all subgroups: $\mathrm{S}^2 = mean(\mathrm{S}_i^2)$.

Note that, if $\overline{\mathrm{X}}_i$ can be approximated by a normal distribution due to the central limit theorem, the control limits in Equation (14) correspond to a $100(1-\alpha)\%$ confidence interval. In

many practical situations, the distribution of features may not be exactly normal. However, it has been shown that the control limits based on the normality assumption can often be successfully used unless the population is extremely non-normal (Montgomery 1997). If the system experienced damage, this would likely be indicated by an unusual number of subgroup means outside the control limits; a charted value outside the control limits is referred to as an *outlier* in this paper. The monitoring of damage occurrence is performed by plotting $\overline{X}_i$ values obtained from the new data set along with the previously constructed control limits.

6. APPLICATION TO CONCRETE COLUMNS

Faculty, students and staff at the University of California, Irvine (UCI) performed quasi-static cyclic tests to failure on seismically retrofitted, reinforced-concrete bridge columns. Vibration tests were performed on the columns at intermittent stages during the static load cycle testing when various amounts of damage had been accumulated in the columns. The associated data obtained from one of the columns are used to investigate the applicability of statistical pattern recognition techniques to vibration-based damage detection problems.

The configuration and dimension of the test column are shown in Figure 1. The test structure was a 137.5 *in* (349 *cm*) long, 24 *in* (61 *cm*) diameter concrete bridge column that was subsequently retrofitted to a 36 *in* (91 *cm*) diameter column. The column was retrofitted by placing forms around the existing column and placing additional concrete within the form. A 24 in^2 concrete block, which had been cast integrally with the column, extends 18 *in* (46 *cm*) above the top of the circular portion of the column. This block was used to attach the hydraulic actuator to the column for quasi-static cyclic testing and to attach the electro-magnetic shaker used for the vibration tests. The column was bolted to the testing floor with 25 *in* (63.5 *cm*) thick in the UCI laboratory during both the static

cyclic tests and vibration tests. The detail of the test structure can be found at http://ext.lanl.gov /projects/damage_id.

6.1 Test Procedure

A hydraulic actuator was used to apply lateral loads to the top of the column in a quasi-static cyclic manner. The loads were first applied in a force-controlled manner to produce lateral deformations at the top of the column corresponding to $0.25\Delta y_T$, $0.5\Delta y_T$, $0.75\Delta y_T$ and Δy_T. Here, Δy_T is the lateral deformation at the top of the column corresponding to the theoretical first yield of the longitudinal reinforcement. The structure was cycled three times at each of these load levels. Next, a lateral deformation corresponding to the actual first yield Δy was estimated based on the observed response. Loads were then applied in a displacement-controlled manner, again in sets of three cycles, at displacements corresponding to $1.5\Delta y$, $2.0\Delta y$, $2.5\Delta y$, etc. until the ultimate capacity of the column was reached.

Vibration tests were conducted on the column in its undamaged state, and after cycling loading at the subsequent displacement levels, Δy, $1.5\Delta y$, $2.5\Delta y$, $4.0\Delta y$, and $7.0\Delta y$. In this study, these vibration tests are referred to as damage level 0 thought 5, respectively. The excitation for the vibration tests was provided by an APS electro-magnetic shaker mounted off-axis at the top of the structure. The shaker rested on a steel plate attached to the top square block of the concrete column. Horizontal loading was transferred from the shaker to the structure through a friction connection between the shaker and the steel support plate. The shaker was controlled in an open-loop manner while attempting to generate 0 - 400 Hz uniform random signal. The RMS voltage level of this signal remained constant during all vibration tests. However, feedback from the column and the dynamics of the mounting plate produced an input signal that was not uniform over the specified frequency range.

6.2 Operational Evaluation

Operational evaluation begins to set the limitations on what will be monitored and how to perform the monitoring as well as tailoring the monitoring to unique aspects of the system and unique features of the damage that is to be detected. Because the test structure was a laboratory specimen, operational evaluation was not conducted in a manner that would typically be applied to an *in situ* structure. However, because the vibration tests were not the primary purpose of this investigation, compromises had to be made regarding the manner in which the vibration tests were conducted. The primary compromise was associated with the mounting of the shaker where it would have been preferable to suspend the shaker from soft supports and apply the input at a point location using a stinger. These compromises are analogous to operational constraints that may occur with *in situ* structures. Environmental variability was not considered an issue because the tests were conducted in a laboratory setting. The available dynamic measurement hardware and software placed the only constraints on the data acquisition process.

6.3 Data Acquisition and Cleansing

Forty accelerometers were mounted on the structure as shown in Figure 1. These locations were selected based on the initial desire to measure the global bending, axial and torsional modes of the column. Note that at locations 2, 39 and 40 the accelerometers had a nominal sensitivity of 10mV/g and were not sensitive enough for the measurements being made. At locations 33, 34, 35, 36, and 37 the accelerometers had a nominal sensitivity of 100mV/g. All other channels had accelerometers with a nominal sensitivity of 1V/g. An accelerometer on the sliding mass of the shaker provided a measure of the input force applied to the column. Analog signals from the accelerometers were sampled and digitized with a Hewlett-Packard 3566A dynamic data acquisition system. Data acquisition

parameters were specified such that 8-second time-histories discretized with 8192 points were acquired. No windowing function was applied to these time histories.

Anti-aliasing filters were applied to further cleanse the data. Analog and digital anti-aliasing filters with cut-off frequencies of 12.8 kHz and 512 Hz, respectively, were used in this study. Data decimation was also used to cleanse the data. Although the data are sampled at 25.6 kHz, the decimation process yields an effective sampling rate of 1.024 kHz. Finally, an AC coupling filter that attenuates signal below 2 Hz was applied to remove DC offsets from the signal. To eliminate high-frequency noise resulting from other experimental activities being conducted in the UC-Irvine Laboratory, the raw time series are passed through an seventh-order Butterworth low-pass filter with a cutoff frequency 150 Hz. These cleansing process significantly improved the quality of data.

6.4 Feature Extraction and Data Compression

The PCA, SPC and projection techniques are illustrated using the vibration test data obtained from the test column shown in Figure 1. First, the applicability of SPC to damage diagnosis problem is demonstrated using single AR coefficient obtained from individual measurement point. Here, the AR coefficients are defined as damaged-sensitive features and the subsequent control chart analysis is conducted using the AR coefficient (Section 6.5). Next, the advantage of projection techniques is investigated. Linear and quadratic projections are introduced to map multi-dimensional AR coefficient space into one-dimensional space to maximize the mean differences between the data sets obtained from the undamaged and damaged classes (Section 6.6). SPC analyses are then conducted on the transformed single-scale feature. Third, PCA is carried out to all response time series for spatial dimensionality reduction prior to feature selection and SPC analysis (Section 6.8). That is, all time series from 39 response points are projected onto the first principal component of the covariance

matrix of the time series. The subsequent feature selection and SPC analyses are performed based on this single time series that is a linear combination of the 39 measured time series.

6.5 Statistical Modeling: X-bar Control Chart using Single AR Coefficient

The 8192 point measured time series are first divided into 512 16-point time-windows, and AR(3) is fit to individual window resulting in 512 sets of AR coefficients. Then, using subgroup size 4, 128 (=512/4) subgroup means are obtained. Figure 2 shows the damage diagnosis results using the first coefficient of the AR(3) model. Time histories from measurement point 1 shown in Figure 1 are used for the construction of the control chart. UCL, LCL, and CL denote the upper and lower control limits, and centerline obtained from the time series of the undamaged structure. The control limits corresponding to a 99% confidence interval are constructed by setting $\alpha = 0.01$ in Equation (14). After the construction of the control limits, damage diagnoses using the X-bar chart are performed for the subsequent damage levels 1 through 5.

Note that the extracted feature τ (the first AR coefficient in this case) is standardized prior to the construction of the X-bar control chart: The mean is subtracted from the feature and the feature is normalized by the standard deviation. Therefore, CL for all figures in this paper corresponds to zero. After establishing the control limits and centerline, features obtained at each damage level are plotted relative to the control limits and centerline obtained from the undamaged data. The outliers, which are samples outside the control limits, are marked by "+" sign in all figures. The features extracted at each damage level are also standardized in the same fashion as before. Note that the mean and standard deviation estimated from damage level 0 are used to normalize data from all the subsequent damage levels.

The diagnosis results using the other AR coefficients are also summarized in Table 1. For this particular example, the third AR coefficient seems most indicative of damage, and the first

coefficient is very insensitive to damage. For damage levels 0 and 1, the numbers of total outliers out of 384 samples are 2 and 1, respectively. (there are three AR coefficients and 128 samples for each AR coefficient. Therefore a total of 384 samples are obtained.) These are equivalent to 0.52% and 0.26% of outliers. Considering the fact that the constructed control limits correspond to a 99% confidence interval, features extracted from the in-control system can still produce approximately 1% of outliers without indicating any damage. Therefore, it is not clear if the system experienced any significant damage at damage level 1 based on the analysis of the X-bar control chart using the individual AR coefficient.

6.6 Statistical Modeling: Control Chart Analysis after Linear or Quadratic Projection

Next, the projection techniques are incorporated into the X-bar control chart. As shown in the previous example, some AR coefficients are more sensitive to damage than the others. Furthermore, constructing separate control charts for each AR coefficient would be time consuming. To overcome these difficulties, the construction of multiple control charts using individual AR coefficient is simplified into a single control chart using one-dimensional transformed feature. In the following examples, the three-dimensional AR coefficients are first projected onto one-dimensional space, and the X-bar chart is constructed based on the transformed feature. In general, the projection onto one-dimension space leads to a loss of information, and classes well separated in the original multi-dimensional space may be strongly overlapped in the projected space. However, by using the Fisher's criterion in Equation (8), the projections are determined to maximize the class separation.

Table 2 shows the results of process monitoring after a linear projection. Comparison of Table 1 and Table 2 clearly reveals the improvement of diagnosis performance. Again, the diagnoses in Table 2 are performed using the time series from measurement point 1. Diagnosis results using the other measurement points are conducted and similar performance improvement is observed.

However, the diagnosis results are not presented because of space limitation. As mentioned earlier, the linear projection may not be the optimal projection in this example because the orders of two class covariance matrices (one from the undamaged case and the other from each damage level) are quite different. In theory, the quadratic projection is the optimal one in a sense of minimizing the error of misclassification. However, no significant performance difference between linear and quadratic projections is observed in this example (see Table 2).

6.7 False Positive Alarm Testing

While it is desirable to have features sensitive to damage occurrence, the monitoring system also needs to be robust against false-positive indication of damage. False-positive indication of damage means that the monitoring system indicates damage although no damage is present. To investigate the robustness of the proposed X-bar control chart against false-positive warning of damage, two separate tests are designed.

In the first test, the time histories obtained from the undamaged state of the test structure are divided into two parts. The first half of the time series is employed to construct the control limits, and the false-positive testing is carried out using the second half of the time series. Note that the original time series are 8-second long with 8192 time points, and each half of the time series is 4-second long with 4096 points. The half of the time series is further divided into 256 sets of 16-point time-windows, and AR(3) is again fit to each time window producing 256 sets of AR coefficients. Next, as mentioned before, four consecutive AR coefficients are grouped together resulting in 64 samples with subgroup size 4. Figure 3 (a) shows the construction of the control limits using the first half of the time series, and the fluctuation of the features extracted from the first half time series are plotted together. Figure 3 (b) presents the false-positive testing using the second half of the time series.

For the second test, the control limits are established using the whole 8-second time histories from the undamaged state of the column, and the false-positive test is conducted using a 2-second time series measured from an independent vibration test of the undamaged column. Figure 3 (c) shows the result of damage diagnoses when the linear projection is applied. For all the cases, the number of outliers are less than or equal to two. Therefore, the two sets of tests presented here have demonstrated that damage diagnosis using the combination of X-bar control chart and projection techniques appears to be robust against false-positive indication of damage for the data studied. Again, similar results are obtained using the quadratic projection.

6.8 Principal Component Analysis

In the previous examples, all damage diagnoses are individually carried out for each measurement points. The PCA conducted on the covariance matrix of 39 response time series indicates that the responses of 39 measurement points are closely correlated. Figure 4 shows that the first principal component alone holds about 30% of total information. Therefore, in the following examples, raw time series from the 39 measurement points are first projected onto the first principal component $\mathbf{v}_1$ as shown in Equation (4). Then, the subsequent feature extraction and X-bar control chart analyses are performed in the same fashion as before. Because the linear and quadratic projections have produced similar results, only the damage diagnosis results after PCA and the linear projection at each damage level are displayed in Figure 5. However, diagnosis results after the quadratic projection are also summarized in Table 3. The results of Table 3 are equivalent to or slightly better than those of Table 2 and much better than those of Table 1. That is, PCA condenses all time series information spatially distributed along the column, and successfully identifies all five damage cases.

7. SUMMARY AND DISCUSSION

A vibration-based damage detection problem is cast in the context of statistical pattern recognition. This statistical approach is used to identify the plastic hinge deformation of a concrete bridge column solely based on the vibration test data. First, the applicability of SPC to the damage diagnosis problem is demonstrated using individual time series from different measurement points. AR models are constructed using the measured time signals, and damage diagnoses using X-bar control charts are performed using an individual AR coefficient as a damage-sensitive feature. The X-bar control chart provides a framework for monitoring changes in the selected feature mean values and for identifying samples that are inconsistent with the past data sets. Next, linear and quadratic projections are introduced to map the multi-dimensional AR coefficients into one-dimensional feature space to maximize the differences in the mean values between the two data sets being compared. The control chart analysis is then conducted on the transformed single dimension feature data. Third, the robustness of the proposed approach against false-positive indication of damage is demonstrated using two separate time histories obtained from the initial test structure. Finally, PCA is carried out on all response time series for spatial dimensionality reduction prior to feature extraction. That is, all time series from multiple measurement points are projected onto the first principal component of the time series covariance matrix, and the subsequent feature selection is performed using this compressed time series.

The projection techniques improved the performance of control chart analysis compared to the damage diagnosis using the individual AR coefficient. When the projection techniques and PCA are combined, the control charts successfully indicated the system response anomaly for all investigated damage levels by showing a statistically significant number of outliers outside the control limits. It should be also noted that this study is carried out in an unsupervised learning mode. Although the projection techniques require two separate data sets, no claim is made that they are

from two different classes. It is only assumed that there is one data set from the undamaged class and the other data set is from an *unknown* class. The ability to apply unsupervised damage detection techniques to civil engineering structures is very important because response data from a similar damaged system are rarely available.

In general, the observation of a large number of outliers in the control chart does not necessarily indicate that the structure is damaged, but only that system has varied to cause a statistically significant change in its vibration response. This variability can be caused by a variety of environmental and operational conditions that the system is subjected to. Because the influence of operational and environmental factors on the dynamic characteristics of the test structure is minimal for the presented laboratory test, the deterioration of the structure was assumed to be the main cause of the abnormal changes of the system. However, operational and environmental conditions such as wind, humidity, intensity and frequency of traffic loading should be taken into account for applications to *in-situ* civil engineering infrastructures. A novel approach to data normalization, combining Auto-Regressive (AR) and Auto-Regressive with eXogenous inputs (ARX) techniques, is developed to explicitly incorporate the environmental and operational conditions into the statistical pattern recognition paradigm so as that the effect of damage on the vibration response could be discriminated from these effects, and to prevent the operational and environmental variability from causing false-positive indications of damage (Sohn et al. 2001).

The presented approach is very attractive for the development of an automated continuous monitoring system because of its simplicity, minimum interaction with users, and a seamless process of continuous data stream analysis. A research effort is underway to integrate the proposed diagnosis algorithm into a sensing unit through a programmable micro-processing chip. The processed data output of these sensing units can be further monitored at a central facility using a wireless

communication system. Because signal processing and damage diagnosis can be conducted independently at an individual sensor level, many issues related to data transmission, such as time synchronization among the multiple sensors, can be simplified. Finally, the only output to the end user will be a simple indication of the structure safety using green, yellow, or red lights. This strategy offers a potential for a significant breakthrough in structural health monitoring technology through an integrated sensing/data interrogation process that has not been attempted to date.

Several issues remain for further study. This study focuses only on the identification of damage existence. Based on personal conversation with bridge field engineers, building owners, bridge managers, and insurance companies, their utmost urgent need for civil infrastructures is mainly to investigate *the presence of damage*. Then, visual inspections or more sophisticated localized nondestructive diagnosis techniques can be applied to pinpoint and quantify structural deterioration. The localization and quantification of damage has not been addressed in this current study. The extension of this approach to damage localization is addressed in Sohn and Farrar (2000).

ACKNOWLEDGEMENT

The funding for this work has come from the Department of Energy's Enhanced Surveillance Program and a cooperative research and development agreement with Kinemetrics Corporation, Pasadena, California. Vibration tests on the columns were conducted jointly with Prof. Gerry Pardoen at the University of California, Irvine using Los Alamos National Laboratory's University of California Interaction Funds. CALTRANS provided the primary funds for construction and cyclic testing of the columns.

REFERENCES

1. Bishop, C. M. (1995). *Neural Networks for Pattern Recognition*, Oxford University Press, Oxford, UK, 1995.
2. Box, G. E. P., Jenkins, G. M., and Reinsel, G. C. (1994). *Time Series Analysis: Forecasting and Control*, Prentice Hall, New Jersy.
3. Brockwell, P. J., and Davis, R. A. (1991). *Time Series: Theory and Methods*, Springer, New York, 1991.
4. Doebling, S. W., Farrar, C. R., Prime, M. B., and Shevitz, D. W. (1998) "A Review of Damage Identification Methods that Examine Changes in Dynamic Properties," *Shock and Vibration Digest*, 30(2), 91-105.
5. Farrar, C. R., and Doebling, S. W. (1999). "Vibration-Based Structural Damage Identification," *accepted for publication of Philosophical Transactions: Mathematical, Physical and Engineering Sciences*, Royal Society, London, UK.
6. Fugate, M. L., Sohn, H., and Farrar, C. R. (2000). "Vibration-Based Damage Detection using Statistical Process Control," *accepted for publication of Mechanical Systems and Signal Processing*, Academic Press, London, UK.
7. Fukunaga, K. (1990). *Introduction to Statistical Pattern Recognition*, Academic Press, New York, NY.
8. Montgomery, D. C. (1997). *Introduction to Statistical Quality Control*, John Wiley & Sons Inc., New York, NY.
9. Scott, D. W. (1992). *Multivariate Density Estimation: Theory, Practice, and Visualization*, John Wiley & Sons Inc., New York, NY.

10. Sohn, H. and Farrar, C. R. (2000). “Time Series Analyses for Locating Damage Sources in Vibration Systems,” *accepted for presentation at International Conference on Noise and Vibration Engineering*, Leuven, Belgium, September 13-15.
11. Sohn, H., Farrar, C. R., and Hunter, N. F. (2001). “Data Normalization Issue for Vibration-Based Structural Health Monitoring,” *accepted for presentation at the 19th International Modal Analysis Conference*, Orlando, FL, February 5-8.
12. Sohn, H., Fugate, M. L., and Farrar, C. R. (2000). “Damage Diagnosis using Statistical Process Control,” accepted for presentation at Conference on Recent Advances in Structural Dynamics, Southampton, UK.

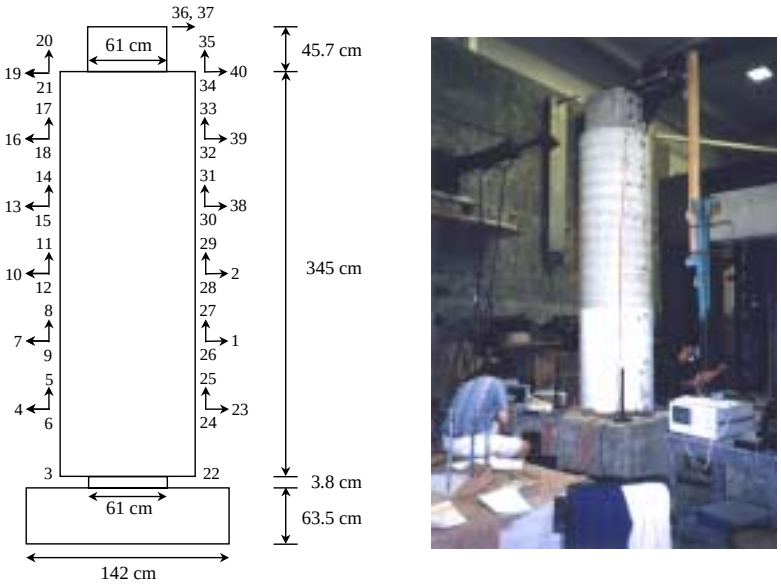

Figure 1: Column dimensions and photo of an actual test structure.

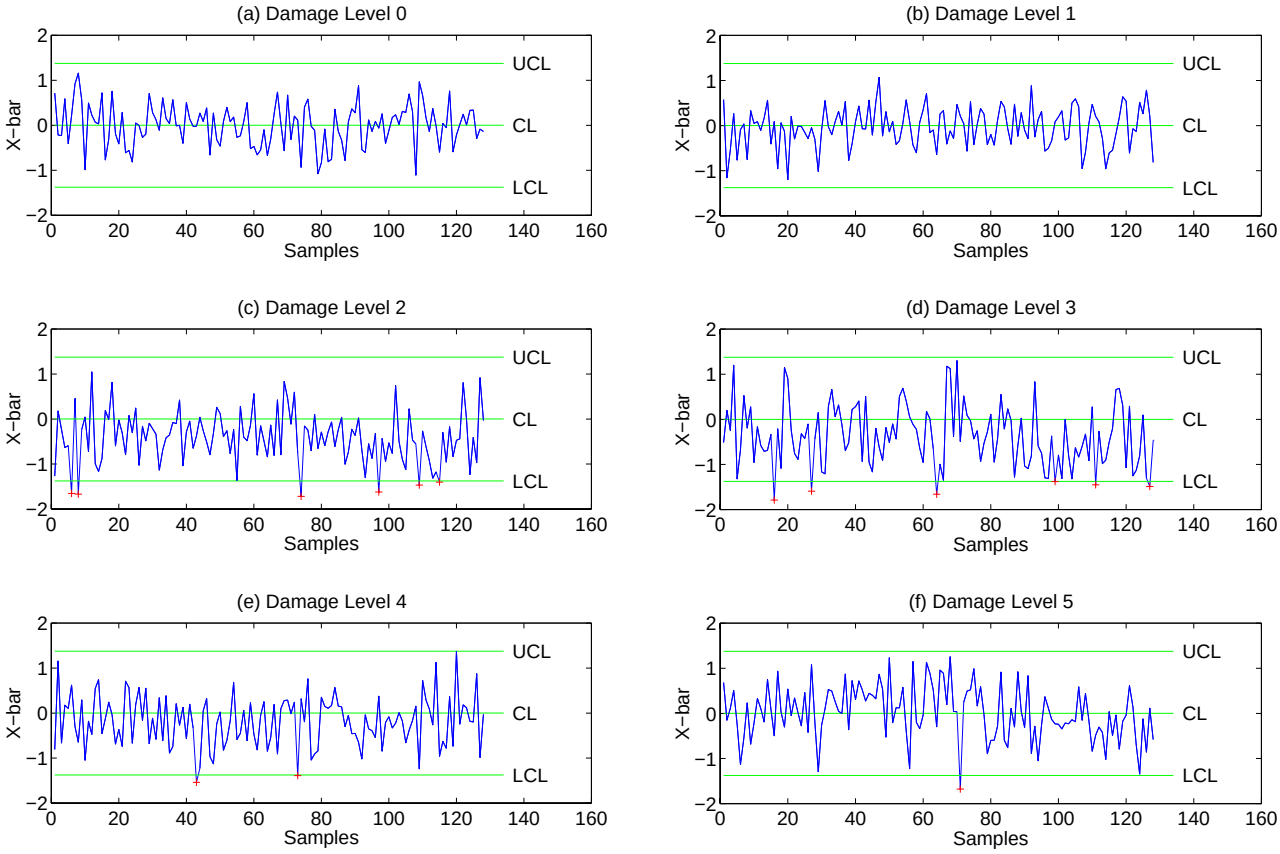

Figure 2: X-bar control chart using the first AR coefficient

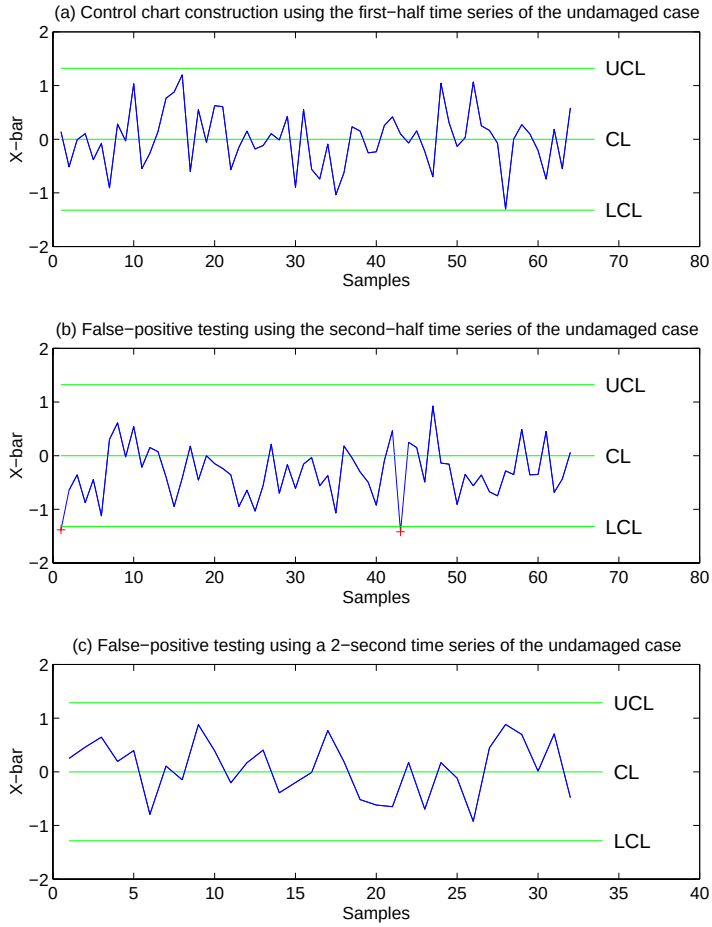

Figure 3: False-positive testing using linear projection

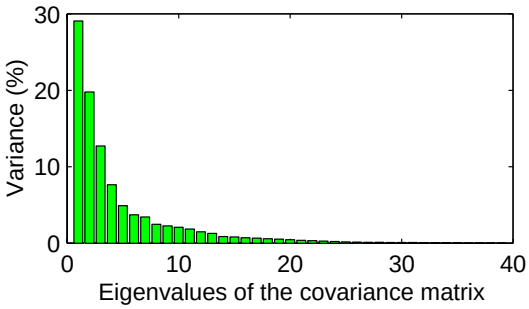

Figure 4: PCA of the covariance matrix of 39 response points

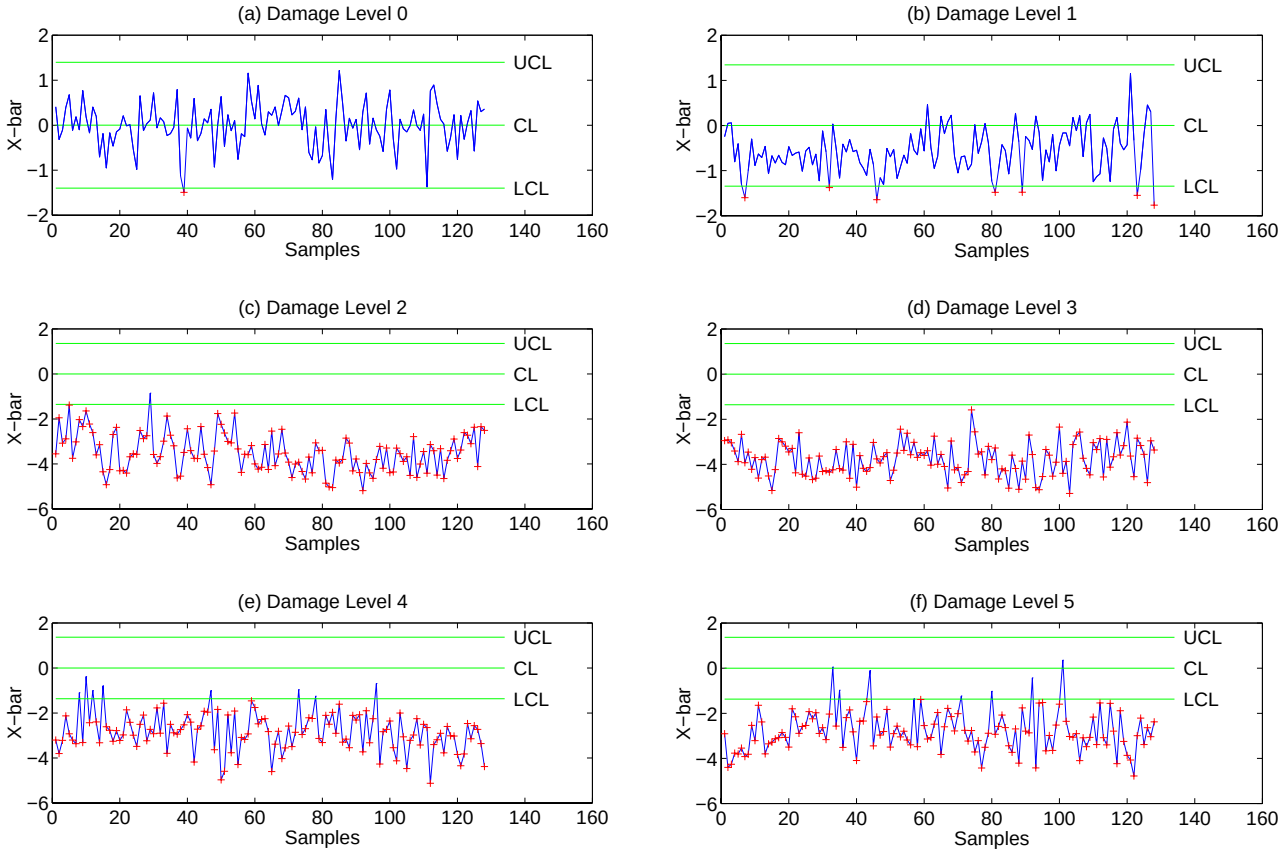

Figure 5: X-bar control chart of the AR coefficients after principal component analysis of all measurement points and linear projection

Table 1: Outlier numbers of X-bar control chart using different AR coefficients

AR coefficient	Damage Level					
	0	1	2	3	4	5
α_1	0/128*	0/128	6/128	6/128	2/128	1/128
α_2	0/128	0/128	6/128	10/128	30/128	23/128
α_3	2/128	1/128	12/128	31/128	77/128	88/128
Total # of outliers	2/384 (0.52%)	1/384 (0.26%)	24/384 (6.25%)	47/384 (12.24%)	109/384 (28.39%)	112/384 (29.17%)

*1/128 indicates that there is a single outlier out of 128 sample data points.

Table 2: Outlier numbers of X-bar control chart using linear or quadratic projection

Projection	Damage Level					
	0	1	2	3	4	5
Linear	1/128*	5/128	24/128	125/128	121/128	127/128
Quadratic	3/128	3/128	34/128	128/128	127/128	128/128

*1/128 indicates that there is a single outlier out of 128 sample data points.

Table 3: Damage diagnosis results after PCA and linear/quadratic projections

Projection	Damage Level					
	0	1	2	3	4	5
Linear	1/128* (0.78%)	7/128 (5.47%)	127/128 (99.22%)	128/128 (100.0%)	120/128 (93.75%)	120/128 (93.75%)
Quadratic	1/128 (0.78%)	7/128 (5.47%)	126/128 (98.44%)	127/128 (99.22%)	121/128 (94.53%)	124/128 (96.88%)

*1/128 indicates that there is a single outlier out of 128 sample data points.